The pH-Dependent Binding of NADH and Subsequent Enzyme Isomerization of Human Liver $\beta_3\beta_3$ Alcohol Dehydrogenase[†,‡]

Carol L. Stone,*[,§] Mary Beth Jipping,[§] Kwabena Owusu-Dekyi,[||] Thomas D. Hurley,[||] Ting-Kai Li,[||] and William F. Bosron[||]

Department of Chemistry and Chemical Biology, Stevens Institute of Technology, Hoboken, New Jersey 07030, and Departments of Biochemistry and Molecular Biology and of Medicine, Indiana University School of Medicine, Indianapolis, IN 46202-5122

Received December 15, 1998; Revised Manuscript Received March 4, 1999

ABSTRACT: Human class I $\beta_3\beta_3$ is one of the alcohol dehydrogenase dimers that catalyzes the reversible oxidation of ethanol. The β_3 subunit has a Cys substitution for Arg-369 (β369C) in the coenzyme-binding site of the β_1 subunit. Kinetic studies have demonstrated that this natural mutation in the coenzyme-binding site decreases affinity for NAD^+ and NADH. Structural studies suggest that the enzyme isomerizes from an open to closed form with coenzyme binding. However, the extent to which this isomerization limits catalysis is not known. In this study, stopped-flow kinetics were used from pH 6 to 9 with recombinant β369C to evaluate rate-limiting steps in coenzyme association and catalysis. Association rates of NADH approached an apparent zero-order rate with increasing NADH concentrations at pH 7.5 ($42 \pm 1\ s^{-1}$). This observation is consistent with an NADH-induced isomerization of the enzyme from an open to closed conformation. The pH dependence of apparent zero-order rate constants fit best a model in which a single ionization limits diminishing rates ($pK_a = 7.2 \pm 0.1$), and coincided with V_{max} values for acetaldehyde reduction. This indicates that NADH-induced isomerization to a closed conformation may be rate-limiting for acetaldehyde reduction. The pH dependence of equilibrium NADH-binding constants fits best a model in which a single ionization leads to a loss in NADH affinity ($pK_a = 8.1 \pm 0.2$). Rate constants for isomerization from a closed to open conformation were also calculated, and these values coincided with V_{max} for ethanol oxidation above pH 7.5. This suggests that NADH-induced isomerization of β369C from a closed to open conformation is rate-limiting for ethanol oxidation above pH 7.5.

Alcohol dehydrogenase catalyzes the NAD^+-dependent reversible oxidation of alcohols (EC 1.1.1.1); addition of coenzyme is a prerequisite to substrate binding. Five classes of alcohol dehydrogenase isoenzymes, active as dimers, have been identified in human tissue (*1*). Class I isoenzymes contain the α, β, and γ subunits, while classes II and III contain the π and χ subunits, respectively. The fourth class, consisting of the σ subunit, is a predominant form in stomach mucosal tissue (*2*).

Heterogeneity of the class I β subunit (*ADH2* polymorphism) exists among racial groups, varying by single amino acid substitutions at positions 47 or 369. Whereas β_1 (Arg 47 and Arg 369) is found predominantly among the Anglo-American population, β_2 (containing His 47 and Arg 369) is found in 85% of the Asian population, and β_3 (Arg 47 and Cys 369) is found in 25% of the African-American population (*3,4*). Individuals heterozygous for the β_3 subunit reportedly metabolize ingested ethanol significantly faster than those individuals who are homozygous for the β_1 subunit (*5*). The $\beta_3\beta_3$ isoenzyme has been implicated in protecting infants of African descent from alcohol-related birth defects (*6*).

The observed rates of ethanol metabolism in humans expressing the β_1 or β_3 subunit of alcohol dehydrogenase correlate with the large differences in steady-state kinetic parameters at pH 7.5 under *in vitro* conditions (*7*). The K_m value for NAD^+ with $\beta_3\beta_3$ is nearly 100 times higher than that with $\beta_1\beta_1$, and the K_m value for ethanol is over 700 times higher. The V_{max} for ethanol oxidation with $\beta_3\beta_3$ is over 30 times faster than that with $\beta_1\beta_1$. Stopped-flow kinetics of the purified enzymes at pH 7.5 reveal that the NADH association rate constant with $\beta_3\beta_3$ is 100 times slower than that with $\beta_1\beta_1$ (*8*). Whereas the rate-limiting step of ethanol oxidation and acetaldehyde reduction with $\beta_1\beta_1$ and $\beta_2\beta_2$ at pH 7.5 is coenzyme dissociation (*9*, *10*), the rate-limiting step with $\beta_3\beta_3$ has not been reported. The stopped-flow kinetics of NADH association and dissociation are presented here.

Comparison of the X-ray crystallographic structures of the human $\beta_3\beta_3$ and $\beta_1\beta_1$ coenzyme-bound complexes reveals little structural difference (*8*). Amino acid position 369 of the two isoenzymes is located in the coenzyme-binding site, in close proximity to the coenzyme pyrophosphate moiety. The position interacts with the pyrophosphate moiety of

[†] This work was supported by R37-AA07117, R37-AA02342, P50-AA07611, and a Scientist Development Award to CLS on K21-AA00148.

* Correspondence should be addressed to Carol L. Stone, Ph.D., Department of Chemistry and Chemical Biology, Stevens Institute of Technology, Castle Point on Hudson, Hoboken, NJ 07030. Phone: 201-216-5544. Fax: 201-216-8240. E-mail: cstone1@stevens-tech.edu.

[‡] Dedicated to Dr. William E. Bradley, Professor of Neurology, University of Washington, Seattle, WA.

[§] Stevens Institute of Technology.

[||] Indiana University School of Medicine, Indianapolis, IN 46202-5122.

10.1021/bi982944v CCC: $18.00
Published on Web 04/13/1999

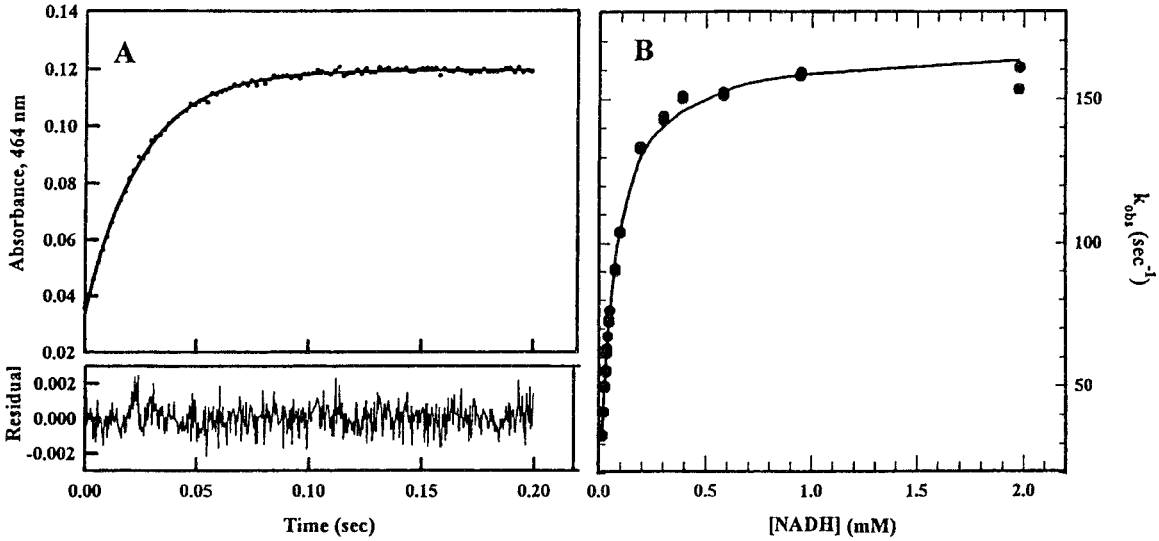

FIGURE 1: Apparent zero-order NADH association rate constants with β369C at pH 6.5. Shown in Figure 1 is the result of an experiment with the enzyme (final concentration of 3 μN) conducted with excess DACA (●), as described in Experimental Procedures. Figure 1A shows the exponential trace of apparent NADH association with the enzyme at a final NADH concentration of 20 μM. Every fifth data point of over 400 is shown. The data fit best a single-exponential equation, with $k_{obs} = 41.1 \pm 0.2$ s^{-1} (solid curve). Figure 1B shows that, with increasing NADH concentrations, the observed rates deviated from linearity, approaching an apparent zero-order rate constant; data fit best the equation $k_{obs} = A[\text{NADH}]/([\text{NADH}] + B)$ (see Experimental Procedures), in which $A = 168 \pm 1$ s^{-1} and $B = 59 \pm 1$ mM. Standard errors for observed rates at 2 mM NADH are slightly visible beyond the data points.

NAD(H) through structured water molecules. One structured water molecule is found between position 369 and the pyrophosphate moiety with $\beta_1\beta_1$, while two additional water molecules are located in the coenzyme-binding site of the coenzyme-bound $\beta_3\beta_3$ isoenzyme (*8*, *11*).

X-ray structure studies with horse liver alcohol dehydrogenase indicate that a conformational change is associated with coenzyme binding (*12*). Studies by Plapp and coworkers (*13*, *14*) and others (*15*−*17*) have suggested with the horse liver enzyme that such a phenomenon may be kinetically significant. This conformational step has been hypothesized to be the rate-limiting step of acetaldehyde reduction with horse alcohol dehydrogenase (*18*), but it has not been tested by direct kinetic methods. We earlier reported evidence of a human $\beta_2\beta_2$ conformational change at pH 10 subsequent to NADH binding (*19*), but evidence of such a phenomenon with $\beta_3\beta_3$ or any other human alcohol dehydrogenase isoenzyme at physiological pH has not been reported.

To explain the role of amino acid position 369 in NADH binding and subsequent enzyme isomerization, we examined stopped-flow kinetics of a site-directed β_1 cDNA mutant containing the Cys 369 that appears in β_3 (β369C)[1] across a wide pH range. We report here that β369C exhibits a measurable apparent zero-order rate at pH 7.5 that is consistent with NADH-induced isomerization of the alcohol dehydrogenase enzyme. We show evidence that this conformational change is rate-limiting for coenzyme release at pH 7.5. The rate-limiting role of this isomerization is also examined for acetaldehyde reduction by β369C.

EXPERIMENTAL PROCEDURES

Enzyme Preparation, Enzyme Stability, and Buffers. The recombinant human $\beta_3\beta_3$ isoenzyme (β369C) was expressed and purified from *Escherichia coli*, as described (*8*, *19*). The recombinant enzyme β369S containing a serine at position 369 was similarly expressed and purified (*20*). The absence of spurious mutations was established.

Enzyme stability was evaluated from pH 5.5 through 10 at 25 °C. For these studies, enzyme (0.3 mg/mL) was incubated in buffer at a given pH, and the enzyme standard activity was measured by sub-sampling at various incubation times. The β369C isoenzyme was judged stable from pH 5.5 through 9 for at least 2 h at 25 °C; kinetic studies were limited to this pH range because stability of the enzyme decreased dramatically above pH 9. The β369S mutant was not stable at 25 °C at any pH value studied (data not shown).

All kinetic studies were examined with a buffer combination of 15 mM PIPES and 15 mM BICINE. This buffer combination resulted in a minimal change in conductivity across the pH range studied (*19*). Enzyme standard activity of $\beta_3\beta_3$ was measured by monitoring the increase in NADH at 340 nm ($\epsilon_{1cm} = 6.22$ mM^{-1}) in a reaction mixture containing 2.4 mM NAD^+ and 66 mM ethanol, in 0.1 M sodium phosphate, pH 7.0, at 25 °C, assuming a specific activity of 5.8 units/mg. One unit of activity reduces one micromole of NAD^+ per minute at 25 °C.

Stopped-Flow Kinetics. Stopped-flow kinetics were performed at 25 °C on either a HITECH SF-51 instrument or an Applied Photophysics SX-18MV instrument. Exponential traces were analyzed with either HITECH or Applied Photophysics software. Linear and nonlinear regressions were analyzed with SAS (Cary, NC), evaluating goodness-of-fit by correlation coefficient or *F*-statistic. All exponential traces fit best a single-exponential model; a sample exponential trace is shown in Figure 1A.

Pseudo-first-order NADH rate association constants were examined using excess 4-*trans*-(*N*,*N*-dimethylamino)-cinnamaldehyde (DACA) as a substrate monitor at 464 nm (*19*). Twelve to 25 data points at final NADH concentrations of 6.6−50 μM NADH were used in the reactions, which

[1] Abbreviations: β369C, expressed recombinant $\beta_3\beta_3$, which contains a Cys 369; β369R, expressed recombinant $\beta_1\beta_1$; DACA, ((*N*,*N*)-dimethylamino)cinnamaldehyde; PIPES, piperazine-*N*,*N*′-bis[2-ethanesulfonic acid]; BICINE, *N*,*N*-bis[2-hydroxyethyl]glycine.

contained final concentrations of 3 μN[2] enzyme and 75 μM DACA. These data fit well a line, the slope of which represented the pseudo-first-order rate constant. Sample correlation coefficients were generally >0.910. Apparent zero-order NADH association rate constants were similarly obtained at final NADH concentrations as high as 3.5 mM. Data were fit to the equation $k_{obs} = A[NADH]/([NADH] + B)$, where B = half-maximal concentration and A = apparent zero-order rate constant. The F-statistics of the 20−35 data points were at least 2231.

Pseudo-first-order and apparent zero-order NADH association rate constants were confirmed by monitoring NADH fluorescence emission through a 400 nm long wavelength pass filter (330 ± 3 nm excitation), eliminating the DACA monitor from the reactions (*19*). The apparent NADH dissociation rate constants were simultaneously obtained (*19*). Data obtained from experiments with 25−60 data points were fit to the equation $k_{obs} = C + A[NADH]/([NADH] + B)$, where B = half-maximal concentration, A = limiting rate constant, and C = NADH dissociation rate constant.

Steady-State Kinetics. The K_i values for NADH (K_i^{NADH}) were evaluated on a Perkin-Elmer Lambda 40 double beam spectrophotometer from pH 6 to pH 9 at 25 °C. Six NAD^+ concentrations (0.18−18 mM) and NADH concentrations (5−1300 μM) were examined at saturating ethanol concentrations of 0.5 M at pH 6 through 7.5, and 1.5 M above pH 7.5. A total of 72−95 data points were evaluated to produce estimates of V_{max} for ethanol oxidation, K_m^{NAD+}, and K_i^{NADH}. Data were analyzed for competitive, uncompetitive, and noncompetitive inhibition mechanisms.

Values of V_{max} for ethanol oxidation, K_m^{NAD+}, and $K_m^{ethanol}$ were also obtained from pH 6 through 9 by varying simultaneously five concentrations of NAD^+ (0.1−1.6 mM) and five concentrations of ethanol. At pH 6 through 7, the concentrations ranged from 0.1 to 1.6 mM NAD^+ and 20 to 150 mM ethanol. At pH 8 through 9, the NAD^+ and ethanol concentrations ranged from 0.5 to 8 mM and 30 to 240 mM, respectively. The 72−95 data points at each pH fit well a sequential mechanism, as judged by F-statistic, residual analysis, and t-statistic for the statistical significance of ethanol estimated parameter (data not shown).

Values of V_{max} for acetaldehyde reduction, K_m^{NADH}, and $K_m^{acetaldehyde}$ were obtained from pH 6.5 through 8.5. Acetaldehyde and NADH were varied simultaneously. At least 87 data points were used in each analysis. Concentrations of NADH ranged from 0.01 to 0.1 mM at pH 6.5, 0.03 to 1 mM at pH 7.5, and 0.1 to 1.4 mM at pH 8.5. Data fit well a sequential mechanism. Acetaldehyde concentrations ranged from 0.1 to 10 mM at pH 6.5, 1 to 200 mM at pH 7.5, and 5 to 250 mM at pH 8.5. Additionally, acetaldehyde reduction was assayed with β369C at 1.66 mM NADH, the maximum amount of NADH detectable in the double beam spectrophotometer. The concentrations of acetaldehyde used at each pH were 10 and 20 mM at pH 6; 65, 50, and 100 mM at pH 7 and 7.5; 0.2 and 0.4 M at pH 8 and 8.5; and 0.6 and 1.2 M at pH 9. Kinetics were performed in a cuvette with a path length of 0.3 cm, monitoring the decrease of NADH over time.

[2] Enzyme concentration is expressed per active site concentration (N). Human $\beta_3\beta_3$ contains two indistinguishable active sites per molecule.

Scheme 1: NADH-Induced Enzyme Isomerization from an Open to Closed Conformation

$$E_{open} + NADH \underset{k_{-1}}{\overset{k_1}{\rightleftharpoons}} E_{open}(NADH) \underset{k_{-2}}{\overset{k_2}{\rightleftharpoons}} E_{closed}(NADH)$$

Calculation of Individual Rate Constants. In experiments with β369C, the observed NADH association rates approached an apparent zero-order, NADH-independent rate constant (Figure 1B). The apparent zero-order rate constants obtained with β369C are consistent with a kinetic model describing a two-step process, in which a first, NADH-dependent step is followed by a second step that is independent of NADH. The proposed NADH-binding sequence is shown in Scheme 1, in which the apparent zero-order rate constant is k_2. The pseudo-first-order NADH rate constants with β369C, assuming the binding sequence shown in the scheme, represents k_2k_1/k_{-1}. Assuming further that the enzyme functions by a sequential mechanism in which coenzyme binds before substrate, K_i^{NADH} values obtained from steady-state kinetics represent $k_{-1}k_{-2}/k_1k_2$, and the ratio of K_i^{NADH} and the pseudo-first-order rate constant produces k_{-2}. A combination of stopped-flow and steady-state kinetics, then, were used to evaluate k_2, k_{-1}/k_1, and k_{-2}.

RESULTS

Apparent NADH Zero-Order and Acetaldehyde Reduction. Observed NADH association rates with β369C ($\beta_3\beta_3$) at final NADH concentrations above 50 mM were not linearly dependent on NADH and approached a zero-order rate of 168 ± 1 s^{-1} that was independent of NADH concentration (Figure 1B). No changes in amplitude were observed, indicating that the phenomenon was not due to inhibitors. Changes in DACA concentration did not affect the observed rates, indicating that the observed rate was not limited by DACA association and dissociation rates. Deviation from linearity was not observed with human liver β369R ($\beta_1\beta_1$) at pH 7.5; observed rates with β369R remained linearly dependent on NADH concentrations to the limits of instrumental detection (about 1200 s^{-1}) (data not shown).

Apparent zero-order rate constants with β369C were obtained from pH 5.5 to 9 (Figure 2). The apparent zero-order rate constant at pH 5.5 was 690 ± 60 s^{-1}, while that at pH 7.5 was reduced an order of magnitude to 42 ± 1 s^{-1}. Above pH 7.5, the apparent rate constants were limited to a rate 30 times less than that at pH 5.5; at pH 9, the rate was 23 ± 1 s^{-1}. The pH dependence of the apparent zero-order rate constants fit best a model in which a single ionization limits diminishing rates (*19*). The resulting F-statistic was 17-fold greater than the fit of the data to a linear model. The pK_a was estimated to be 7.2 ± 0.1. Apparent rate constants determined in the presence of excess DACA were confirmed at pH 7.5 by extrinsic enzyme (tryptophan) fluorescence, as described in Experimental Procedures. The apparent zero-order rate constant obtained at this pH, by two independent experiments, produced rates of 24.5 ± 5.4 and 26.3 ± 4.5 s^{-1}, values that were not statistically significant from the rate constant of 33 s^{-1} determined from the fitted curve.

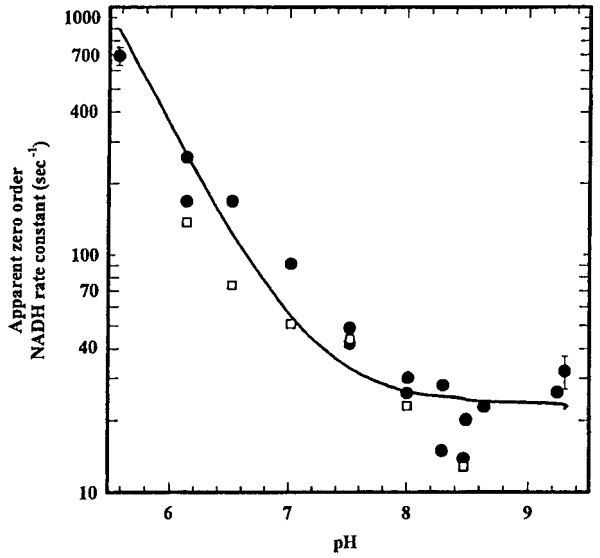

FIGURE 2: The pH dependence of apparent zero-order NADH association rate constants with β369C. The pH dependence of apparent zero-order NADH rate constants with β369C is shown (●). Most standard error bars do not reach beyond the data points. The data fit best a model in which a single ionization limits the pH-dependent decrease in observed rate constants, $r = \check{r}(1 + H^+/K_a)$ (solid curve), in which r is the apparent rate constant at any pH, and $\check{r}$ is the limiting rate; $\check{r} = 23.4 \pm 1.1\ s^{-1}$ and $pK_a = 7.2 \pm 0.1$. Kinetic assays of acetaldehyde reduction, described in Experimental Procedures, are also shown (□).

Steady-state kinetic constants for acetaldehyde and NADH with β369C were obtained at pH 6.5, 7.5, and 8.5. The K_m for NADH varied from 0.10 ± 0.02 mM at pH 6.5 to 0.28 ±0.03 mM at pH 7.5 and increased dramatically to 3.2 ± 1.6 mM at pH 8.5. The K_m for acetaldehyde varied from 1.1 ± 0.2 mM at pH 6.5 to 4.9 ± 0.6 at pH 7.5. At pH 8.5, the K_m for acetaldehyde was 44 ± 38 mM. Although saturating NADH concentrations could not be obtained above pH 7.5, assays of acetaldehyde reduction at 1.6 mM NADH with saturating concentrations of acetaldehyde coincided with the pH dependence of apparent zero-order rate constants at all other pH values (Figure 2).

Pseudo-First-Order Rate Constants. At final NADH concentrations below 50 μM, the observed NADH association rates with β369C were approximately linearly dependent on NADH concentration (Figure 3A). The pH dependence of these pseudo-first-order rate constants is shown in Figure 3B for β369C (circles and solid line). From pH 5.5 to pH 6.5, the pseudo-first-order rate constants for β369C were about 2 s^{-1}. Above pH 6.5, the rate constant dropped precipitously to a value of $0.010 \pm 0.001 s^{-1}$ at pH 9.2. The data fit best a model in which a single ionization with a pK_a of 6.8 ± 0.1 leads to a drop in pseudo-first-order rate constants. The pH dependence of the pseudo-first-order rate constants previously reported for β369R fit a similar curve (dashed curve; ref *19*). The rate constants with β369R, however, were at least 4 times faster across the pH range studied, and the pK_a value was shifted to 8.1 ± 0.2.

Apparent Equilibrium Dissociation Constants for NADH. The pH dependence of the apparent NADH-binding constant (k_{-1}/k_1) with β369C is shown in Figure 4. Each data point in the figure was calculated from the NADH pseudo-first-order and apparent zero-order rate constants, as described in Experimental Procedures. Below pH 7.5, the calculated value for (k_{-1}/k_1) was about 0.1 mM; this value increased an order of magnitude from pH 7.5 to 9.2; at pH 9.2 the calculated binding constant was over 2 mM. The instability of the enzyme above pH 9 precluded analysis at higher pH values; however, the pH-dependent pattern of the available data fit best a model in which a single ionization leads to a loss in NADH affinity for β369C. The pK_a of this ionization was estimated to be 8.1 ± 0.2.

Equilibrium NADH-Binding Constants. Estimates of K_i^{NADH} with alcohol dehydrogenase are obtained from steady-state kinetics by varying NAD^+ and NADH concentrations simultaneously at saturating ethanol concentrations. These K_i^{NADH} values represent the equilibrium NADH-binding constant (K_{eq}^{NADH} or k_{-1}/k_1), with enzymes that function by a sequential mechanism, in which NAD^+ binding precedes ethanol binding, and the mode of inhibition by NADH is competitive (*21*). If an internal isomerization is inserted into

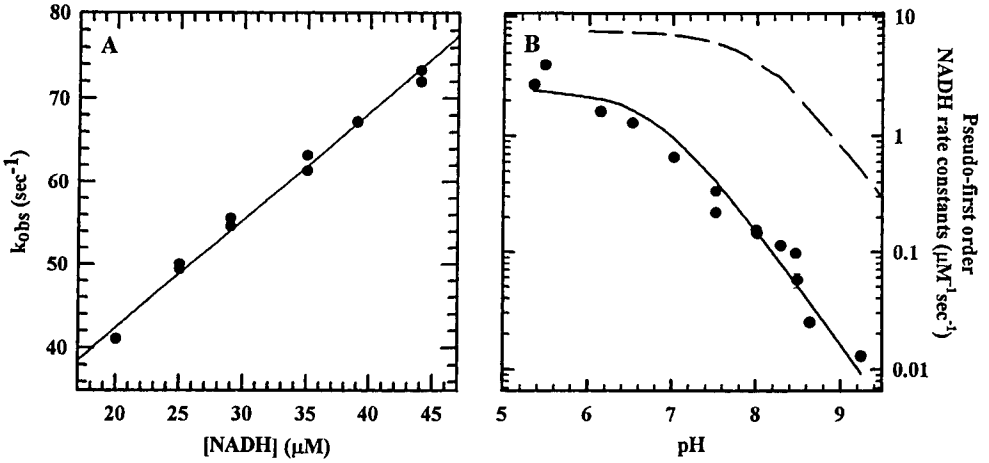

FIGURE 3: Pseudo-first-order NADH association rate constants with β369C. At NADH concentrations below 50 μM, observed rates increased linearly with NADH concentration. Panel A shows the results of a linear regression at pH 6.5 containing a final DACA concentration of 75 μM. Data fit the equation $k_{obs} = k_{first-order}[NADH] + y$ (solid line), in which $k_{first-order} = 1.29 \pm 0.04\ \mu M^{-1}\ s^{-1}$, and y, the intercept, is $16.6 \pm 1.3\ s^{-1}$ (sample correlation coefficient = 0.99). Panel B shows the pH dependence of the pseudo-first-order rate constants obtained for β369C (●). Data fit best a model in which a single ionization leads to a drop in pseudo-first-order rate constants, $r = \check{r}/(1 + K_a/H^+)$, in which r is the rate constant at any pH, and $\check{r}$ is the limiting rate (solid curve); $pK_a = 6.8 \pm 0.1$ and $\check{r} = 2.55 \pm 1.25\ s^{-1}$. The apparent rate constants obtained previously with β369R are also shown (dashed curve), producing $pK_a = 8.1 \pm 0.2$ (*19*).

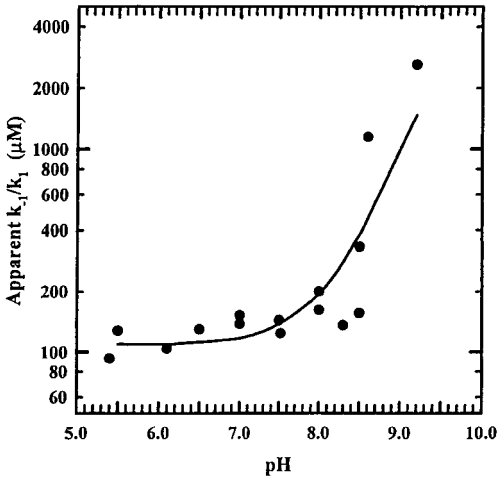

FIGURE 4: The pH dependence of NADH equilibrium dissociation constants with β369C. Estimates of k_{-1}/k_1 with β369C were calculated from apparent NADH zero-order rate constants and pseudo-first-order rate constants (circles) (see Experimental Procedures). Data fit best a model in which the equilibrium dissociation constant was governed by a single ionization, $r = \check{r}(1 + K_a/H^+)$ (solid curve), in which r is the value of the constant at any pH, and $\check{r}$ is the limiting constant; $pK_a = 8.1 \pm 0.2$ and $\check{r} = 110 \pm 1$ s^{-1}.

Table 1: Values of K_i^{NADH} with β369C, 25 °C[a]

pH	K_i^{NADH} (μM)	*F*-statistic[b]	*p* value[c]
6.1	9.8 ± 0.9	4201	<0.01
7.0	22 ± 2	5905	<0.01
7.5	46 ± 4	4238	<0.01
8.0	48 ± 3	4243	<0.01
8.5	150 ± 10	11234	<0.01
8.9	610 ± 50	5055	<0.10

[a] Estimates are shown with the standard error of the fit. [b] *F*-statistic shown is that obtained by fitting the data to competitive inhibition. [c] Level of significance for the ratio of the *F*-statistics derived from competitive versus noncompetitive fits. The *F*-statistics derived from fits to uncompetitive inhibition were at least 2-fold lower than the *F*-statistic derived from fits to competitive inhibition.

the sequence mechanism (see Scheme), the mode of inhibition remains competitive, but the K_i^{NADH} value is now composed of a combination of rate steps, ($k_{-1}k_{-2}/k_1k_2$).

The K_i^{NADH} value for β369C was studied at varying pH values (Table 1). The K_i^{NADH} values increased 4-fold from pH 6.1 to 8.0, and the values increased dramatically above pH 8 to over 600 at pH 8.9. Across the pH range studied, the competitive mode of inhibition clearly predominated over other possible inhibition modes. This result is consistent with a reaction sequence mechanism that follows a sequential mechanism.

Apparent NADH Dissociation Rate Constants and Ethanol Oxidation. From the K_i^{NADH} estimates obtained by steady-state kinetics and the pseudo-first-order rate constants obtained from stopped-flow kinetics, the pH dependence of k_{-2} was calculated with β369C (Table 2). The values of k_{-2} varied with increasing pH from 7 to 29 s^{-1}.

The pH dependence of apparent NADH dissociation rates was obtained by fluorescence stopped-flow kinetics (Table 2). These rates did not differ statistically from pH 6 to 7.5, varying between about 20 and 44 s^{-1}. Above pH 7.5, the observed rates became unreliable; amplitudes became indiscernible from the background. Assuming the mechanism in Scheme 1, apparent NADH dissociation rates represent the limiting rate of either k_{-1} or k_{-2}. At pH 6, 7, and 7.5, these rates coincided with calculated k_{-2} values.

Table 2: The pH Dependence of NADH Dissociation Constants with β369C, 25 °C

pH	k_{-2} (s^{-1})[a]	app. $NADH_{off}$ (s^{-1})[b]	V_{max}^{ox} (s^{-1})[c]
6.1	20	44 ± 12	2.98 ± 0.15
7.0	29	22 ± 2	3.67 ± 0.32
7.5	21	26 ± 4	3.17 ± 0.25
8.0	7	nr	7.50 ± 0.62
8.5	7	nr	9.80 ± 0.63
8.9	12	nr	15.7 ± 3.3

[a] k_{-2} values were calculated from K_i^{NADH} values and NADH pseudo-first-order rate constants. [b] Apparent NADH dissociation rate constants were obtained by fluorescence as described in Experimental Procedures. Estimates are shown with the standard error of the fit: nr, kinetic estimates were not reproducible. [c] V_{max} values for ethanol oxidation were obtained by steady-state kinetics as described in Experimental Procedures. Estimates are shown with the standard error of the fit.

Values of V_{max} for ethanol oxidation were obtained across a wide pH range (Table 2). From pH 6 to 7.5, the V_{max} was approximately constant, at about 3−3.5 s^{-1}. Above this pH value, the V_{max} increased with increasing pH. At pH 8.9, the V_{max} was 15.7 (± 3.3) s^{-1}, a value 5 times higher than that at lower pH values. The values of V_{max} at and below pH 7.5 were nearly 10-fold lower than the estimates for k_{-2}. Above pH 7.5, however, the V_{max} values coincided well with the calculated values of k_{-2}.

DISCUSSION

A combination of steady-state and stopped-flow kinetics was used to identify the individual rate constants that govern NADH binding to β369C and the extent to which this limits ethanol oxidation and acetaldehyde reduction from pH 6−9. This recombinant human class I β alcohol dehydrogenase contains a Cys for Arg substitution at position 369. The recombinant protein represents the natural β_3 subunit expressed in 25% of the African-American population. The $\beta_3\beta_3$ isoenzyme exhibits the highest V_{max} and K_m values for ethanol and NAD^+ of any Class I alcohol dehydrogenase. We describe in this paper a rate-limiting apparent zero-order rate with NADH association to β369C. This indicates that NADH association to human alcohol dehydrogenase $\beta_3\beta_3$ occurs in two steps: an initial coenzyme recognition and a subsequent NADH-induced enzyme isomerization (Scheme) that is independent of NADH concentration. The kinetics are not consistent with a scheme where enzyme isomerization is followed by coenzyme binding, because product inhibition profiles with NAD^+ and NADH were competitive (Table 1). Also, those experiments performed with DACA demonstrate that there is no change in amplitude with increasing NADH concentrations and DACA will only bind to a productive binary complex (*19*). Therefore, we conclude that the data presented here are most consistent with two steps, in which an initial NADH-binding event is followed by a concentration-independent event.

The first, concentration-dependent step in NADH binding with $\beta_3\beta_3$ (k_1 and k_{-1} in Scheme 1) is dependent on a substituent with a pK_a value of about 8.1 (Figure 4). Several theories have been suggested to explain the pH dependence of coenzyme binding to horse and human alcohol dehydro-

genase enzymes. Adolph and co-workers (*8*) suggested with horse alcohol dehydrogenase that the pH dependence observed with the first NADH-binding step is actually defined by the net charge of the protein, a hypothesis first proposed by Lively and co-workers (*22*). This hypothesis predicts that $\beta_1\beta_1$ and horse alcohol dehydrogenase, with Arg at positions 47 and 369, could be more attractive to NADH than $\beta_2\beta_2$, with a His at position 47, or $\beta_3\beta_3$, with a Cys at position 369. Pseudo-first-order NADH rate constants at pH 7.5 of 8.9 ($\pm$ 0.6), 3.7 ($\pm$ 0.4), and 0.48 ($\pm$ 0.03) s^{-1} with $\beta_1\beta_1$, $\beta_2\beta_2$, and $\beta_3\beta_3$, respectively, support this hypothesis (Figure 3B; ref *19*).

The pK_a of 8.1 observed in Figure 3 with $\beta_3\beta_3$ for initial NADH binding is consistent with the deprotonation of a cysteine residue such as Cys 369. As Burnell and co-workers have pointed out (*3*), an electrostatic repulsion of NADH by the thiolate ion formed by the deprotonation of Cys-369 would occur at pH values above pH 8. This is consistent with the increase in k_{-1}/k_1 seen above this pH. Studies with β369S, a mutant that contains the neutrally charged serine at position 369, were inconclusive, because the enzyme was not stable at 25 °C during the 3−4 h needed for kinetic experiments. The results presented here indicate that amino acid position 369 is involved in the initial NADH-binding step. The difference between $\beta_1\beta_1$ (with an Arg at position 369) and $\beta_3\beta_3$ in pseudo-first-order NADH association rates (Figure 3B) suggests that a positive charge at position 369 is important for high-affinity NADH binding.

After the initial NADH-binding step, human $\beta_3\beta_3$ may wrap itself around the coenzyme molecule as the result of NADH-induced isomerization (k_2 and k_{-2} in Scheme 1). This hypothesis is supported by the appearance of an apparent zero-order rate constant that limits NADH association rates (Figure 1B). Evidence of the zero-order rate constant was reproducibly observed with β369C across the pH range studied by both substrate absorbance and enzyme tryptophan fluorescence techniques. The apparent zero-order rate constants were obtained with low millimolar concentrations of NADH at rates easily detectable with our stopped-flow apparatus.

With horse alcohol dehydrogenase, Adolph and co-workers (*15*) stated that NADH association approaches an apparent zero-order rate constant of about 1200 s^{-1}. We saw similar results with $\beta_1\beta_1$ and $\beta_2\beta_2$ at pH 7.5. We are reluctant, however, to attribute this observation to a rate constant because the rate is very close to the limits of detection with our stopped-flow instrument (1200−1500 s^{-1}). We were unable to definitively assign enzyme isomerization as a kinetically significant step in coenzyme binding with $\beta_1\beta_1$ and $\beta_2\beta_2$. Apparent zero-order rate constants would have to be at least 1200 s^{-1} at pH 7.5. This rate would be about 300 times faster than the V_{max} for acetaldehyde reduction with $\beta_1\beta_1$, suggesting that the step is kinetically insignificant at this pH. Evidence of a zero-order isomerization step was reported for NADH binding to $\beta_2\beta_2$ only at high pH (*19*).

The pH dependence of an open to closed conformation with β369C is consistent with mediation by a single ionizable group, with a pK_a of 7.2 ($\pm$ 0.1) (Figure 2B), that limits the rate of isomerization when deprotonated. These data are consistent with the pH dependence observed by Sekhar and Plapp (*14*), using NAD^+ binding to the horse liver alcohol dehydrogenase. The NADH-induced isomerization step is most likely to be influenced by charged groups close to the coenzyme-binding site. These dynamics must prepare the active site for substrate binding and "charge" the catalytic zinc. Substituents such as His51 (*23*), or Lys228 (*24*), have been suggested to mediate coenzyme binding to horse alcohol dehydrogenase. The data reported here cannot address either possibility, although site-directed mutagenesis studies at position 51 with human alcohol dehydrogenase isoenzymes have been investigated, and the results suggest that substitutions at this position do not significantly influence coenzyme binding (*10*).

Amino acid position 369 may function as a mediator of coenzyme binding. The Cys for Arg-369 substitution with β369C certainly affects the rate of NADH-induced isomerization. At pH 7.5, the value of k_2 with the mutant enzyme is 42 ($\pm$ 0.4) s^{-1} (Figure 2B). The same rate step with $\beta_1\beta_1$ is at least 1200 s^{-1}, a value nearly 30 times faster than that with the β369C. Water molecules in the coenzyme-binding site near position Cys369 appear to play an integral role in binding (*8*). Moreover, comparison of the X-ray crystal structures of coenzyme-bound horse alcohol dehydrogenase and the apo-enzyme indicate that at least 12 structured water molecules are displaced from the coenzyme-binding site during coenzyme binding (T. Hurley, personal communication). Desolvation may play a role in enzyme isomerization, but there is not enough structural information of the apo-isoenzymes to identify water definitively as a mediator in coenzyme binding.

It has been suggested that zinc-bound water in the active site mediates coenzyme binding to horse alcohol dehydrogenase (*25*−*28*). If the water molecule mediates coenzyme binding with $\beta_3\beta_3$, then the pK_a of the water molecule would be shifted far down to 7.2 with NADH association. It would suggest that deprotonation of the water molecule leads to a slower rate of enzyme isomerization.

The rate-limiting step in NADH association is the concentration-independent step represented by k_2. Dissociation of NADH is governed by one of two concentration-independent steps, k_{-2} or k_{-1}. A comparison of apparent $NADH_{off}$ rates and calculated k_{-2} rates suggests that k_{-2} is the rate-limiting step in NADH dissociation with β369C at pH 7.0 and 7.5 (Table 2). This suggests that k_1 and k_{-1} play a minor role in NADH binding relative to isomerization. At pH 7.5, the V_{max} for ethanol oxidation with $\beta_3\beta_3$ is about 3.2 s^{-1} (Table 2), a value nearly 7 times slower than k_{-2}, the rate of enzyme isomerization from the closed to open conformation. At and above pH 8, however, the values calculated for k_{-2} coincide with V_{max} for ethanol oxidation, indicating that k_{-2} may be rate-limiting in this pH range.

The V_{max} for acetaldehyde reduction with $\beta_3\beta_3$ is reportedly about 40 s^{-1} at pH 7.5 (*7*), a value very close to that of k_2. The rate of acetaldehyde reduction from pH 6 to 8 coincided well with predicted values of k_2 (Figure 2B). These data suggest that the isomerization of the binary complex to form a closed enzyme−coenzyme complex may be at least partially rate-limiting for acetaldehyde reduction. The apparent rate of acetaldehyde reduction at pH 8.5 probably underestimates the actual rate under saturating NADH and acetaldehyde conditions because experiments were limited to 1.6 mM NADH, a concentration that is subsaturating for β369C at this pH. In contrast, the rate-limiting step of acetaldehyde reduction with $\beta_1\beta_1$ and $\beta_2\beta_2$ is reported to be

coenzyme release (*9*). Hardman proposed, on the basis of steady-state kinetics, that the rate-limiting step of acetaldehyde reduction with horse liver alcohol dehydrogenase is coenzyme isomerization (*18*), a hypothesis also suggested by Cook and Cleland (*29*). Our data are the first to directly indicate that the enzyme isomerization step is rate-limiting with a human alcohol dehydrogenase isoenzyme.

This pH-dependent study of NADH binding to recombinant human $\beta_3\beta_3$ (β369C) by stopped-flow kinetics and steady-state kinetics indicates that amino acid position 369 is involved in initial recognition, as well as in a subsequent NADH-induced isomerization step. The data presented here indicate that this isomerization step from the open to closed conformation may be the rate-limiting step of acetaldehyde reduction by the enzyme. In addition, isomerization of the enzyme from the closed to open conformation is the rate-limiting step of NADH release, and may be the rate-limiting step of ethanol oxidation above pH 7.5.

ACKNOWLEDGMENT

We would like to thank Mary Ann Gerke, Colleen Harden, and Steve Parsons for producing the enzyme and Ann Kusnadi for preparing the β369S expression vector. We also thank Sandra Roberts and Monica Jain for technical assistance.

REFERENCES

1. Edenberg, H., and Bosron, W. F. (1997) in *Comprehensive Toxicology* (Guengerich, F., Ed.) Vol. 3: Biotransformation, pp 119−131, Pergamon, New York.
2. Stone, C. L., Thomasson, H. R., Bosron, W. F., and Li, T.-K. (1993) *Alcohol.: Clin. Exp. Res. 17* (4), 911−918.
3. Burnell, J. C., Carr, L. G., Dwulet, F. E., Edenberg, H. J., Li, T.-K., and Bosron, W. F. (1987) *Biochem. Biophys. Res. Commun. 146*, 1227−1233.
4. Burnell, J. C., and Bosron, W. F. (1989) in *Human metabolism of alcohol* (Crow, K. E., and Batt, R. D., Eds.) Vol. II, pp 65−75, CRC Press, Boca Raton, Florida.
5. Thomasson, H. R., Beard, J. D., and Li, T.-K. (1995) *Alcohol.: Clin. Exp. Res. 19*, 1494−1499.
6. McCarver, D. G., Thomasson, H. R., Martier, S. S., Sokol, R. J., and Li, T.-K. (1997) *J. Pharmacol. Exp. Ther. 283* (3), 1095−1101.
7. Burnell, J. C., Li, T. K., and Bosron, W. F. (1989) *Biochemistry 28*, 6810−6815.
8. Davis, G. J., Bosron, W. F., Stone, C. L., Owusu-Dekyi, K., and Hurley, T. D. (1996) *J. Biol. Chem. 271* (29), 17057−17061.
9. Stone, C. L., Hurley, T. D., Amzel, L. M., Dunn, M. F., and Bosron, W. F. (1993) in *Enzymology and Molecular Biology of Carbonyl Metabolism* (Weiner, H. C. D., Flynn, T. J., Ed.) Vol. 4, pp 429−437, Plenum Press Inc., New York.
10. Davis, G. J., Carr, L. G., Hurley, T. D., Li, T.-K., and Bosron, W. F. (1994) *Arch. Biochem. Biophys. 311* (2), 307−312.
11. Hurley, T. D., Bosron, W. F., Stone, C. L., and Amzel, L. M. (1994) *J. Mol. Biol. 239*, 415−429.
12. Eklund, H., and Branden, C.-I. (1979) *J. Biol. Chem. 254*, 3458−3461.
13. Plapp, B. V., Sogin, D. C., Dworschack, R. T., Bohlken, D. P., Woenckhaus, C., and Jeck, R. (1986) *Biochemistry 25*, 5396−5402.
14. Sekhar, V. C., and Plapp, B. V. (1988) *Biochemistry 27*, 5082−5088.
15. Adolph, H. W., Kiefer, M., and Cedergren-Zeppezauer, E. (1997) *Biochemistry 36*, 8743−8754.
16. Geeves, M. A., and Fink, A. L. (1980) *J. Biol. Chem. 255*, 3248−3250.
17. Dalziel, K. (1963) *J. Biol. Chem. 238*, 2850−2858.
18. Hardman, M. J. (1981) *Biochem. J. 195*, 773−774.
19. Stone, C. L., Bosron, W. F., and Dunn, M. F. (1993) *J. Biol. Chem. 268* (2), 892−899.
20. Kusnadi, A. (1989) Master's thesis, Department of Biochemistry and Molecular Biology, Indiana University, Indianapolis, IN.
21. Segel, I. H. (1975) *Enzyme Kinetics. Behavior and analysis of rapid equilibrium and steady-state enzyme systems*, John Wiley & Sons, New York.
22. Lively, C. R., Feinberg, B. A., and McFarland, J. T. (1987) *Biochemistry 26*, 5719−5725.
23. Eftink, M. R., and Bystrom, K. (1986) *Biochemistry 25*, 6624−6630.
24. Pettersson, G., and Eklund, H. (1987) *Eur. J. Biochem. 165*, 157−161.
25. Andersson, P., Kvassman, J., Olden, B., and Pettersson, G. (1984) *Eur. J. Biochem. 144*, 317−324.
26. Kvassman, J., and Pettersson, G. (1979) *Eur. J. Biochem. 100*, 115−123.
27. Andersson, P., Kvassman, J., Lindstrom, A., Olden, B., and Pettersson, G. (1981) *Eur. J. Biochem. 113*, 425−433.
28. Andersson, P., Kvassman, J., Lindstrom, A., Olden, B., and Pettersson, G. (1980) *Eur. J. Biochem. 108*, 303−312.
29. Cook, P. F., and Cleland, W. W. (1981) *Biochemistry 20*, 1805−1817.

BI982944V